Subcellular compartmentation of different lipophilic fluorescein derivatives in maize root epidermal cells

David Brauer*, Joe Uknalis, Ruth Triana, and **Shu-I Tu**

Plant Soil Biophysics Research Unit, Agricultural Research Service, U.S. Department of Agriculture, Wyndmoor, Pennsylvania

Received September 5, 1995
Accepted January 25, 1996

Summary. Fluorescence microscopy offers some distinct advantages over other techniques for studying ion transport processes in situ with plant cells. However, the use of this technology in plant cells has been limited by our lack of understanding the mechanisms that influence the subcellular distribution of dyes after loading with the lipophilic precursors. In this study, the subcellular distribution of 5-(and 6-)carboxydichlorofluorescein (CDCF), carboxy-SNAFL-1, and carboxy-SNARF-1 was compared to that of 2′,7′-bis-(2-carboxyethyl)-5-(and 6-)carboxyfluorescein (BCECF) after incubation of maize roots with their respective lipophilic precursors. Previously, we reported that incubation of roots with BCECF-acetomethyl ester (BCECF-AM) led to vacuolar accumulation of this dye. Similar results were found when roots were incubated with CDCF-diacetate. In contrast, carboxy-SNAFL-1 appeared to be confined to the cytoplasm based on the distribution of fluorescence and the excitation spectra of the dye in situ. On the other hand, incubation of roots with carboxy-SNARF-1-acetoxymethyl acetate yielded fluorescence throughout the cell. When the cytoplasm of epidermal cells was loaded with the BCECF acid by incubation at pH 4 in the absence of external Ca, the dye was retained in the cytoplasm at least 3 h after the loading period. This result indicated that vacuolar accumulation of BCECF during loading of BCECF-AM was not due to transport of BCECF from cytoplasm to vacuole. The esterase activities responsible for the production of either carboxy-SNAFL-1 or BCECF from their respective lipophilic precursor by extracts of roots were compared. The characterization of esterase activities was consistent with the subcellular distribution of these dyes in root cells. The results of these experiments suggest that in maize root epidermal cells the subcellular distribution of these fluorescein dyes may be determined by the characteristics of the esterase activities responsible for hydrolysis of the lipophilic precursor.

* Correspondence and reprints: Plant-Soil Biophysics Research Unit, Eastern Regional Research Center, ARS, U.S. Department of Agricultures, 600 E. Mermaid Lane, Philadelphia, PA 19118, U.S.A.

Keywords: Cytosolic; Esterase; Fluorescence microscopy; Intracellular compartmentation; Vacuole.

Abbreviations: BCECF (BCECF-AM) 2′,7′-bis-(2-carboxyethyl)-5-(and 6-)carboxyfluorescein (its acetoxymethyl ester) BTB bis-tris-propane; CDCF (CDCF-DA) 5-(and 6-)carboxy-2′,7′-dichlorofluorescein (its diacetate derivative); DAPI 4′,6-diamidino-2 phenylindole dihydrochloride; DMSO dimethylsulfoxide; HEPES N-[2-hydroxyethyl] piperazine-N′-[2-ethanesulfonic acid]; MES 2-[N-morpholino]ethane-sulfonic acid; SNAFL-1 (SNAFL-1-DA) carboxyl SNAFL-1 (its diacetate); SNARF-1 (SNARF-1-AM) carboxyl SNARF-1 (its acetoxymethyl acetate).

Introduction

According to the current understanding of Mitchell's chemiosmotic hypothesis, electrochemical gradients produced by P-type and V-type of H^+-ATPases are linked to the influx of nutrients to the cytoplasm and exclusion of toxicants (Sze 1985). In addition, both of these proton pumps are involved in pH regulation of the cytoplasm (Kurkdjain and Guern 1989, Raven and Smith 1979). Both the P-type and V-type ATPases share a common characteristic: they couple the chemical energy from the hydrolysis of ATP to the efflux of protons from the cytoplasm (Sze 1985, Tu et al. 1992). The biochemistry of these two transport H^+-ATPases differs considerably (Nelson and Taiz 1989, Sze 1985, Tu et al. 1992).

The use of fluorescence microscopy after loading pH sensitive dyes into either the cytoplasm or vacuole by the use of lipophilic precursor appears to be a technique that has advantages over previous methods. Fluorescence microscopy should have greater spatial

as to the series of cellular events that have transpired during treatment. Treatment with BrdU may also be useful in studies of plants treated with herbicides in determining the degree of inhibition of DNA synthesis during the treatment, without the use of radiolabelled nucleotides.

Acknowledgements

Thanks are extended to Ms. Lynn Libous-Bailey for technical assistance, to Dr. L. Hickok for spores, and to Drs. K. S. Renzaglia, R. J. Smeda, R. Turley, D. Ferguson, and T. D. Sherman for constructive comments/suggestions on this study. Mention of a trademark, proprietary product, or vendor does not constitute a warranty by the USDA nor does it endorse this product to the exclusion of other products that may be suitable.

References

Åstrom H (1992) Acetylated alpha-tubulin in the pollen tube microtubules. Cell Biol Int Rep 16: 871–881

Cleary AL, Hardham AR (1988) Depolymerization of microtubule arrays in root tip cells by oryzalin and their recovery with modified nucleation patterns. Can J Bot 66: 2353–2366

Gundersen GG, Kalnoski MH, Bulinski JC (1984) Distinct populations of microtubules: tyrosinated and non-tyrosinated alpha tubulin are distributed differentially in vivo. Cell 38: 779–789

Gunning BES, Sammut M (1990) Rearrangements of microtubules involved in establishing cell division planes start immediately after DNA synthesis and are completed just before mitosis. Plant Cell 2: 137–145

Hepler PK (1972) Differential inhibition of cell division in microspores of *Marsilea* with colchicine and isopropyl N-phenylcarbamate. J Cell Biol 55: 112a (abstract)

Hoffman JC, Vaughn KC (1994) Mitotic disrupter herbicides act by a single mechanism but vary in efficacy. Protoplasma 179: 16–25

– – (1995a) Post translational tubulin modifications in spermatogenous cells of the pteridophyte *Ceratopteris richardii*. Protoplasma 186: 169–182

– – (1995b) Using the developing spermatogenous cells of *Ceratopteris* to unlock the mysteries of the plant cytoskeleton. Int J Plant Sci 15: 346–358

– – Joshi HC (1994) Structural and immunocytochemical characterization of microtubule organizing centers in pteridophyte spermatogenous cells. Protoplasma 179: 146–160

James SW, Lefebvre PA (1988) Mutants resistant to anti-microtubule herbicides map to a locus on the uni linkage group in *Chlamydomonas reinhardtii*. Genetics 118: 141–147

– Siflow CD, Stroom P, Lefebvre PA (1993) A mutation in the alpha1 tubulin gene of *Chlamydomonas reinhardtii* confers resistance to anti-microtubule herbicides. J Cell Sci 106: 209–218

Kerr GP, Carter JV (1988) Microtubules of higher plants contain acetylated alpha tubulin. J Cell Biol 107: 670a (abstract)

Kozminski KG, Diener DR, Rosenbaum JL (1993) High level expression of nonacetylatable alpha-tubulin in *Chlamydomonas reinhardtii*. Cell Motil Cytoskeleton 25: 158–170

LeDizet M, Piperno G (1986) Cytoplasmic microtubules containing acetylated alpha tubulin in *Chlamydomonas reinhardtii*: spatial arrangements and properties. J Cell Biol 103: 13–22

Lehnen LP, Vaughn KC (1991) Immunofluorescence and electron microscopic investigations of the effects of dithiopyr on onion root tips. Pestic Biochem Physiol 40: 58–67

Myles DG, Hepler PK (1982) Shaping of the sperm nucleus in *Marsilea*: a distinction between factors responsible for shape generation and shape determination. Dev Biol 90: 238–252

Vaughn KC, Lehnen LP (1991) Mitotic disrupter herbicides. Weed Sci 39: 450–457

– Sherman TD, Renzaglia KS (1993) A centrin homologue is a component of the multilayered structure in bryophytes and pteridophytes. Protoplasma 175: 58–66

Webster DR, Borisy GG (1989) Microtubules are acetylated in domains that turn over slowly. J Cell Sci 92: 58–66

and time resolution than ^{31}P-NMR and assays based on the accumulation of radioactive weak bases and acids (Kurkdjain et al. 1985; Kurkdjain and Guern 1981, 1989; Pfeffer et al. 1987; Roberts et al. 1980). In addition, possible complications arising from the elicitation of a wounding phenomenon in response to impaling by a microelectrode is avoided with fluorescence microscopy.

However, the use of these fluorescent probes to study the biochemistry of plants by light microscopy has been limited by an understanding of the fate of the lipophilic precursor and their corresponding dyes within plant cells. The entrapment of the active dye in mammalian cells is dependent upon esterase activity that converts the lipophilic precursor to the dye (Haugland 1992). Plant cells also contain an abundance of esterase activity, however, these activities may be localized in the vacuole or cytoplasm (Boller and Kende 1979). Therefore, the fate of dyes in plant cells can be different from that observed in mammalian cells for which the probes were developed. For example, the initial experiments with the Ca-sensitive dye, Quin-2, illustrate how a probe that worked well in mammalian systems was unable to detect changes in intracellular Ca when applied to plant cells (Bush and Jones 1990, Cork 1986). A theory that has been formulated to account for differences between plant and mammalian cells in the subcellular distribution of fluorescence dyes hypothesizes that fluid-phase endocytosis or transport of dyes across the tonoplast membrane by anion carrier may be responsible for the delivery of hydrophilic dyes to vacuoles (Oparka 1991).

Recently, Brauer et al. (1995) reported that incubating roots of maize seedlings with the lipophilic precursor of BCECF led to selective accumulation of the dye within the vacuoles of roothair cells. These results were quite unexpected since BCECF was developed to measure cytoplasmic pH in mammalian cells (Haugland 1992) and has been used previously to monitor changes in cytoplasmic pH in plant cells (Dixon et al. 1989, Sakano et al. 1992, Yin et al. 1993). However, Rost et al. (1995) and Slayman et al. (1994) working with the fungi *Pisolithus tinctorius* and *Neurospora crassa*, respectively, have reported the vacuolar accumulation of BCECF when incubated in the presence of BCECF-AM. In this report, we have compared the accumulation of other fluorescein based dyes to that of BCECF to understand the factors that may be responsible for dye entrapment in maize roots.

Material and methods

Growth conditions

2- to 3-day-old seedlings of corn cultivars (FRB 73 from Illinois Foundation Seed Co. and W7551 from Custom Farm Seed Co.) were grown on paper moistened with 0.1 mM $CaCl_2$ (Nagahashi and Baker 1984).

Loading of roots with dyes

The apical 3 to 4 cm of roots were excised from seedlings and placed in 20 ml of pH 6 perfusion buffer, containing 0.2 mM $CaSO_4$, 50 mM glucose and 10 mM MES titrated to pH 6.0 with BTP. The solution was continuously bubbled with air. The lipophilic precursors, SNARF-1-AM, BCECF-AM, CDCF-DA, or SNAFL-1-DA were dissolved in DMSO. Typically, roots were incubated in the presence of 3.0, 5.9, 4.4, or 5.0 µM BCECF-AM, SNAFL-1-DA, SNARF-1-AM, or CDCF-DA, respectively. The DMSO concentration in the loading solution was either less than or equal to 1% of the total solution volume. This concentration of DMSO has been found not to have a measurable effect on cell viability or metabolism (Pfeffer et al. 1987). After 10 to 60 min of incubation at room temperature, roots were rinsed three times for 2 min each in 0.1 mM $CaCl_2$. Roots were then held until observed (<2 h) in aerated pH 6.0 perfusion buffer. The nuclei of root cells were labeled in vivo with DAPI (Lawrence and Possingham 1986) or SYTO-16 stain (Haugland 1992).

Except for DAPI, all dyes and their lipophilic precursors were obtained from Molecular Probes, Inc. (Eugene, OR, U.S.A.). For SNARF-1, SNARF-1-AM, SNAFL-1, SNAFL-1-DA, BCECF, BCECF-AM, CDCF, CDCF-DA, Cl-NERF, DM-NERF, and SYTO-16, the catalog numbers are C-1270, C-1271, C-1255, C-1256, B-1151, B-1150, C-368, C-369, C-2204, D-2202, and S-7572, respectively. DAPI, as well as most of the other reagents, were of the highest purity available from Sigma Chemical Co. (St. Louis, MO, U.S.A.).

To load fluorescein dyes into the cytoplasm, excised root segments were incubated in 50 mM K-phthalate (pH 4.0) containing 12 to 20 µM BCECF, SNAFL-1 or SNARF-1 for 30 to 60 min at 18 to 22 °C. After which, root segments were placed in pH 6 perfusion buffer. Distribution of the dyes was determined by fluorescence microscopy as described below after 30 to 120 min incubation in the pH 6 perfusion buffer. Experiments to determine root tissue viability by in vivo ^{31}P nuclear magnetic resonance were performed essentially as described previously by Pfeffer et al. (1987).

Phase contrast and fluorescence microscopy

Root epidermal cells are visualized with a Nikon Diaphot inverted microscope equipped with long working distance phase contrast lens. Most images were gathered from an area immediately towards the root apex from the region that roothair cells first appeared (Fig. 1). Sample chambers were fashioned from plastic petri dishes by etching out a slot on the bottom and then cementing a 22 × 22 mm 1.5 thickness coverslip to close the opening. Roots were then positioned over the coverslip and held in place with the aid of a small amount of modeling clay. When the fluorescence from standard solutions containing dyes was determined, 400 µl of liquid was placed over the coverslip window and covered with a second coverslip to provide a uniform depth of solution.

For maximum intensity, the fluorescence from BCECF, CDCF, Cl-NERF or DM-NERF was visualized by using excitation and emis-

sion filters with band passes of 473–496 nm and 515–545 nm, respectively. For maximum fluorescence, excitation and emission filters passing wavelengths of 536–556 nm and in excess of 590 nm, respectively, were used to visualize SNAFL-1 and SNARF-1. Fluorescence from DAPI and SYTO-16 stains were visualized with an excitation beam of 365 ± 10 and 470 ± 20 nm, respectively, and emission barrier filter of 400 and 520 nm, respectively.

Both phase contrast and fluorescent images were captured using a charge-coupled device (CCD) camera (587 × 384 pixels) cooled to –45 °C (Photometrics, Ltd.) controlled by IPLab-Spectrum-PMI software (Signal Analysis Corp., version 2.4) and later analyzed by the same software. Light intensities were assigned values between 48 and 4096 and displayed on a grey scale of 256 shades. Histograms plotting pixel frequency as a function of light intensity were utilized to optimize the contrast within images.

Excitation spectra of dyes within the labeled root cells were obtained using an Olympus IMT-2 inverted microscope interfaced with an FM-2010 fluorescence microscope system (Photon Technology Inc., Princeton, NJ, U.S.A.). In this system, a monochromator is used to select the excitation wavelength. For SNARF-1-AM, CDCF-DA, and BCECF-AM loaded root segments, a dichroic mirror of 505 nm was used to deliver the excitation wavelengths to the sample and an emission filter of 535 ± 20 nm was used to select the emitted light. For SNAFL-1-DA loaded cells, a dichroic mirror of 540 nm was used to deliver the excitation light and a barrier filter of 590 nm was used to select the emitted light. The fluorescence from a single epidermal cell was selected by four positional slit adjustments in the light path and detected by photomultiplier tube. These conditions were used to examine a portion of the excitation spectra that was pH dependent. These conditions did not necessarily optimize fluorescence intensity.

Esterases assays

Roots from 3-day-old seedlings were homogenized in 0.25 M sucrose containing 5 mM dithiothreitol and 50 mM HEPES (pH 7.5). Large particulate and debris were removed by straining through cheesecloth and centrifuging at 12,000 **g** for 10 min. The resulting supernatant was used as the crude enzyme preparation. Preparation and storage was at 0 to 4 °C. Protein concentration of enzyme preparation was determined by a modification of the Lowry protocol using bovine serum albumin as a standard (Bensadoun and Weinstein 1976).

The degradation of BCECF-AM to BCECF and SNAFL-1-DA to SNAFL-1 was followed fluorimetrically. 20 to 30 µl of crude extract were diluted to 2.0 ml with either 50 mM MES (titrated to pH 5.5 with BTP) or 50 mM HEPES (titrated to pH 7.5 with NaOH). To this solution, 1 to 40 µl of 0.12 mM BCECF-AM in DMSO were added. The time-dependent production of BCECF was followed by the increase in fluorescence using excitation and emission wavelength of 440 ± 3 and 535 ± 10 nm, respectively. Similarly, the conversion of SNAFL-1-DA was followed by increase in fluorescence using excitation and emission wavelengths of 514 ± 5 and 660 ± 20 nm, respectively, and a stock solution containing 0.2 mM SNAFL-1-DA in DMSO. These excitation and emission wavelengths were selected because the fluorescence intensities of these two dyes were independent of pH at these wavelengths (Haugland 1992).

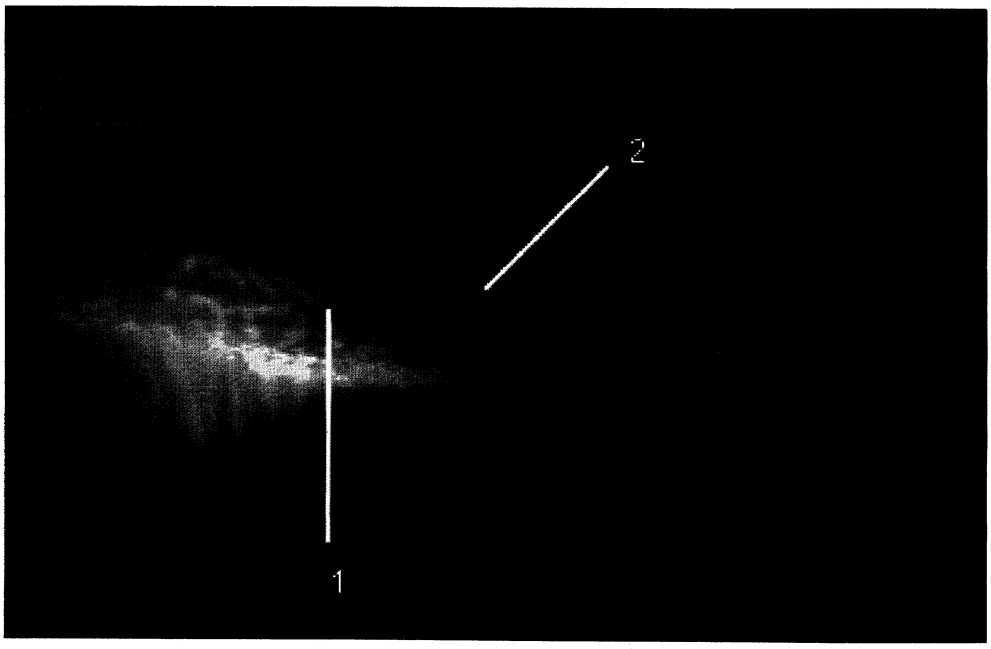

Fig. 1. The distribution of fluorescence along the longitudinal axis of a root after incubation in the presence of BCECF-AM. Roots were incubated in the presence of BCECF-AM for 30 min and then rinsed for 30 min as described in Material and methods. Fluorescence images were produced as described in Material and methods and recorded on Ektachrome film (ASA 400) with the aid of a Nikon UFX-DX camera controller. Arrows *1* and *2* refer to the roothair region and an immediately adjacent epidermal region towards the rootcap, respectively. The entire field represents an area of 1.8 × 1.2 mm

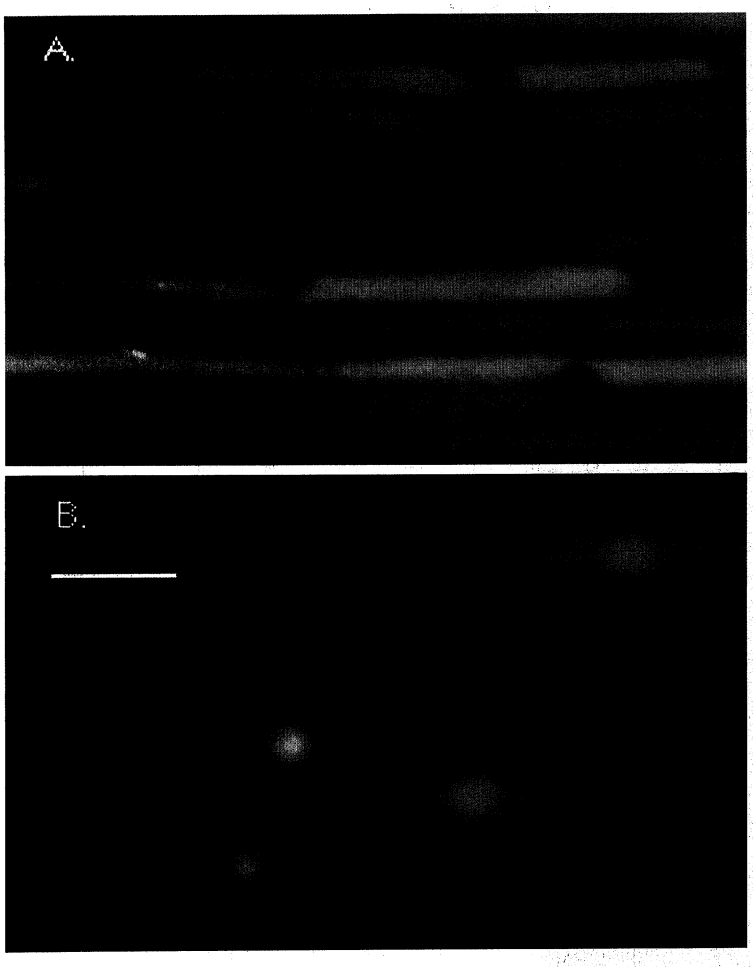

Fig. 2. Subcellular distribution of fluorescence in root epidermal cells after incubation in BCECF-AM. Roots were incubated in the presence of BCECF-AM for 30 min and rinsed for 30 min as described in Material and methods. Fluorescence images of epidermal cells from the two regions of the root identified in Fig. 1 were captured using a cooled CCD camera and IPLAB-Spectrum software: **A** epidermal region without roothairs towards the rootcap roothairs, **B** immediately adjacent roothair region. Bar, for A and B: 10 μm

Results

Localization of BCECF, CDCF, SNAFL-1 and SNARF-1 in root cells

An overview of the longitudinal distribution of BCECF fluorescence after root segments were incubated in the presence of BCECF-AM is presented in Fig. 1. As reported previously by our laboratory (Brauer et al. 1995), the greatest fluorescence intensity was associated with that portion of the root that contained fully developed roothair cells. However, rootcap cells and epidermal cells adjacent to the area where roothair cells first appeared (indicated by arrow 2 in Fig. 1) were also fluorescent. Closer examination of the roothair and epidermal area adjacent to it revealed that a large portion of the cell volume was fluorescent (Fig. 2). The cell's periphery was not labeled, however. Quite often there was a small lobe of the cell's periphery that extended towards the cell's interior that was not fluorescent. When BCECF-AM loaded cells were also labeled with the nucleic acid stain, DAPI, it was this area, unlabeled by BCECF-AM, that became fluorescent (data not shown). Similar results were obtained with another nucleic acid stain, SYTO-16 (data not shown). Therefore epidermal cells from both region appeared to accumulate the BCECF in the vacuole. When the subcellular compartmentation of dyes was studied, epidermal cells from region 2 were imaged because the absence of roothair projections resulted in less out of focus light and sharper images.

When roots were incubated in the presence of CDCF-DA, a labeling pattern similar to that observed with BCECF-AM was obtained (Fig. 3 A). The only possible difference between epidermal cells labeled with CDCF-DA and BCECF-AM was the abundance of small vesicles within the cytoplasm containing dye. The occurrence of these labeled vesicles was noted previously after BCECF-AM labeling (Brauer et al. 1995). However, the abundance of these vesicles in Fig. 3 A was significantly greater than that observed previously after BCECF-AM labeling.

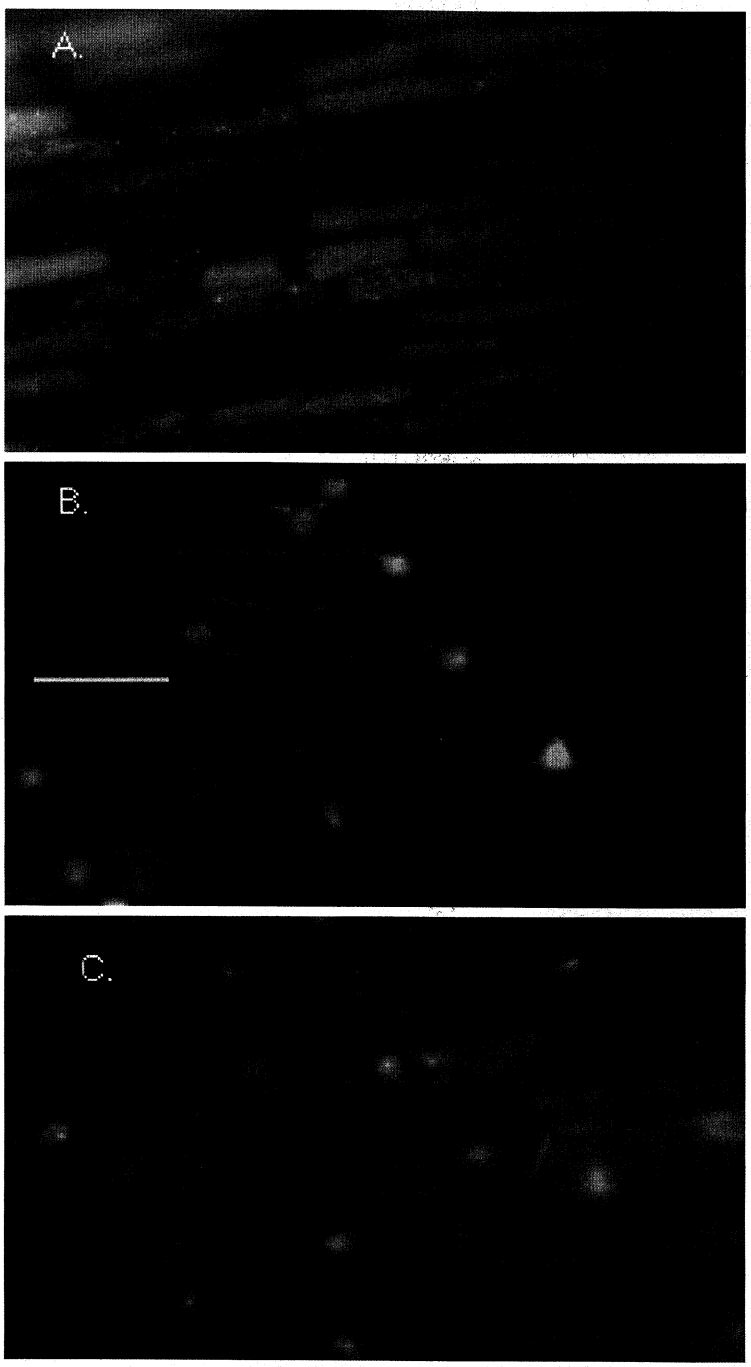

Fig. 3 A–C. Subcellular distribution of fluorescence after incubation of maize roots in different lipophilic precursors of fluorescein derivatives. Maize roots were incubated 30 min in the presence of CDCF-DA (**A**), SNAFL-DA (**B**), and SNARF-AM (**C**) and then rinsed 30 min as described under Material and methods. Fluorescent images were obtained as described under Material and methods using a cooled CCD camera. Bar, for A–C: 10 μm

Quite a different pattern of fluorescence was obtained after incubating roots in the presence of SNAFL-1-DA (Fig. 3 B). There was a striking similarity between the distribution of fluorescence after exposure to SNAFL-1-DA and after staining nucleic acids with either DAPI or SYTO-16, suggesting that SNAFL-1-DA led to cytoplasmic labeling. The fluorescence intensity of SNAFL-1 was quite high in the nucleus and possibly the nucleolus. Image ratio analysis of the nucleic region indicated that the fluorescence intensity reflected a greater amount of SNAFL-1 rather than a change in the pH environment of the dye (data not shown). These results may indicate that SNAFL-1 binds to some nucleic material, although supporting data are lacking at present.

The fluorescence pattern after incubation with SNARF-1-AM was intermediate between that obtained with SNAFL-1-DA and BCECF-AM (Fig. 3 C). A

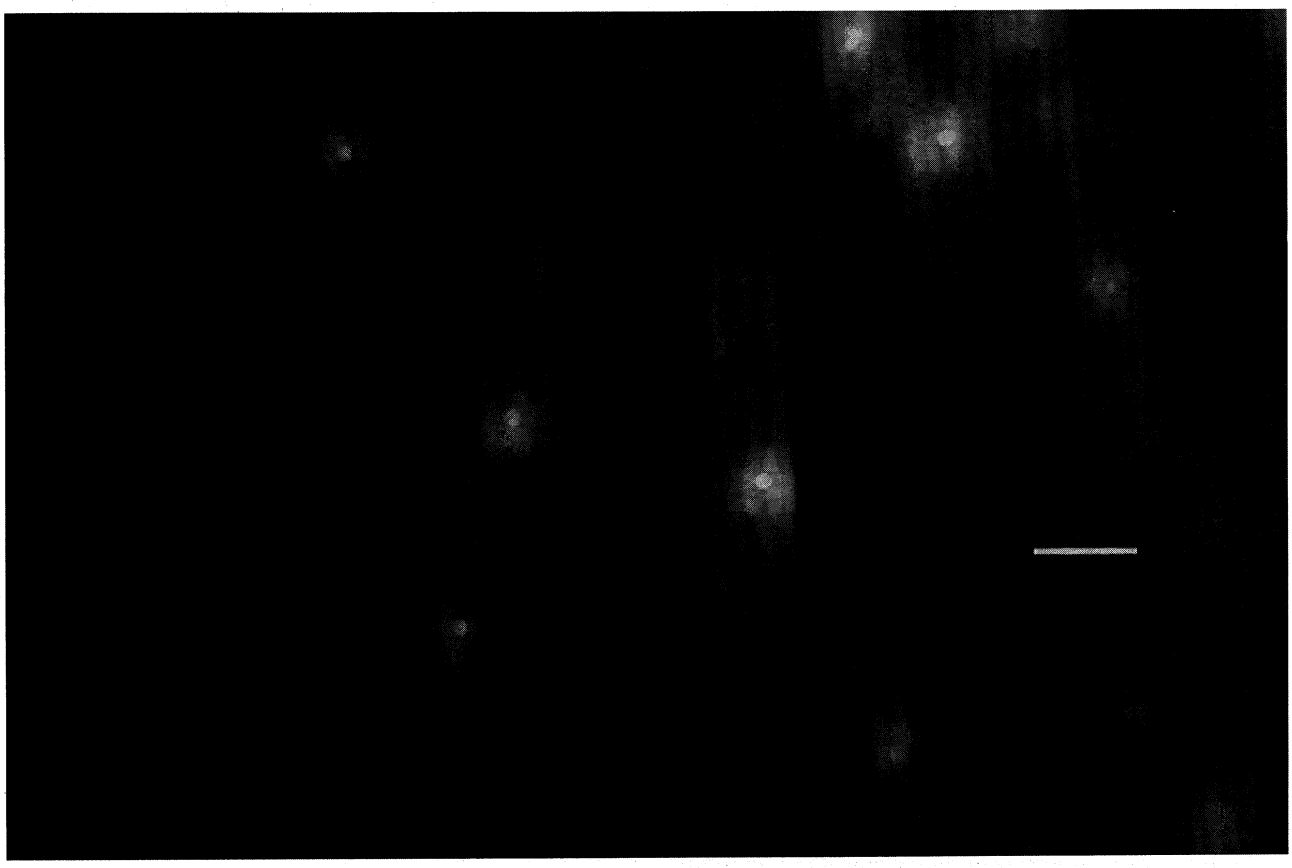

Fig. 4. Subcellular localization of BCECF 3 h after acid loading. Roots were incubated in the presence of 12 μM BCECF in pH 4 phthalate buffer as described under Material and methods for 30 min and then transferred to pH 6 perfusion buffer for 180 min. Fluorescence images were recorded and presented as described under Material and methods. Bar: 10 μm

vast majority of the cell volume was fluorescent with SNARF-1-AM. However, there were areas of more intense fluorescence associated with the cell periphery and the lobular areas.

One important observation concerning the fluorescence of cells loaded with any of these dye precursors was that the subcellular distribution of fluorescence persisted from the initial detection of fluorescence until hours after the loading period (data not shown). That is, if the dye was predominantly in the vacuole during and immediately after the loading period, then the same pattern was observed at least 3 h later in the absence of the lipophilic precursor. In the case of BCECF-loaded roots, the vacuolar localization of BCECF persisted for at least 12 h (data not shown).

Acid loading of fluorescein dyes

When root segments were incubated in the presence of BCECF, SNAFL-1, SNARF-1, Cl-NERF, or NERF-DM in 50 mM K-phthalate (pH 4.0), the epidermal cells became fluorescent. The fluorescence persisted when the roots were removed from the pH 4 buffer and incubated in pH 6 perfusion for at least 2 h. The fluorescein dyes mentioned above were confined to the cytoplasm when loaded in the pH 4 medium (data not shown). Virtually all of the dye remained in the cytoplasm hours after the loading period as exemplified by the results in Fig. 4 with BCECF loaded roots. The pattern of fluorescence from BCECF introduced into the cells by acid loading was very similar to that observed by loading of SNAFL-1 by its lipophilic precursor in Fig. 3. The greatest fluorescence intensity was associated with the nucleus and possibly the nucleoli. Image ratio analysis of the fluorescence pattern indicated that the differences in intensity in Fig. 4 were not due to a change in the pH environment of the dye but rather its dye concentration (data not shown). As in the case of SNAFL-1, the possibility thus exists that BCECF binds to yet unidenti-

fied nuclear material. The metabolism of roots after acid loading in pH 6 perfusion buffer was the same as of untreated roots as determined by in vivo ^{31}P NMR (data not shown). In addition, ^{31}P NMR revealed two inorganic phosphate pools differing in pH, consistent with the maintenance of cytosolic and vacuolar compartments after acid loading. Therefore there was no evidence for the transport of BCECF localized in the cytoplasm to the vacuole, rather BCECF present in the cytoplasm remained in that subcellular compartment. In addition, epidermal cells that were loaded with BCECF into their cytoplasm at pH 4 retained their ability to accumulate dye in the vacuole upon incubation in the presence of BCECF-AM (data not shown).

Excitation spectra of dyes in root cells

The excitation spectrum for the fluorescence emitted from cells loaded with BCECF-AM had a broad peak between 460 and 490 nm. As the excitation wavelength was increased from 490 to 500 nm, there was a decline in the fluorescence intensity. Such a spectrum was very similar to that of BCECF in pH 5 buffer (Fig. 5 A). The fluorescence of CDCF in standard solutions was characterized by a progressive increase in intensity as the excitation wavelength was increased from 400 to 500 nm (Fig. 5 B). There was little if any effect of pH on fluorescence intensity at excitation wavelengths below 420 nm. Above 420 nm, there was progressively greater fluorescence at pH 6 than at pH 5. Above pH 6, there was little change in the fluorescence intensity of CDCF (data not shown). The excitation spectra of CDCF in epidermal cells were more similar to that of the dye at pH 6 than at pH 5.

The excitation spectrum for the fluorescence emitted from cells loaded with SNARF-1-AM had a predominant peak centered about 475 nm and a smaller, distinct peak centered about 424 nm (Fig. 5 C). The excitation spectra from these cells more closely resembled that of the dye in standard solutions with acidic pH values than that of the dye in standard solutions of neutral or alkaline pH values. The fluorescence intensity of SNAFL-1-DA loaded cells was relatively constant as the excitation wavelength was increased from 490 to about 520 nm (Fig. 5 D). As the excitation wavelength was increased from 520 to 530, there was a slight decrease in fluorescence intensity. The broadness of the 490 to 520 nm peak in excitation spectrum of SNAFL-1 in standard solutions decreased as the pH of the solution was lowered. The relative broadness of the excitation peak of SNAFL-1-AM loaded cells indicated that the pH environment of the dye was slightly alkaline. The comparison of the excitation spectra of roots labeled with SNAFL-1, SNARF-1, CDCF, and BCECF to that of the corresponding dyes in standard solutions of differing pH indicated that BCECF, CDCF, and SNARF-1 were localized in an acidic environment in loaded cells whereas the SNAFL-1 in loaded cells was in a neutral or slightly alkaline environment. These results based on the pH environment of the dyes were consistent with those obtained from examining the subcellular distribution of the fluorescence in Figs. 2 and 3.

Esterase activity

The distribution of the dye within maize root cells appeared to be determined by the localization of the esterase that hydrolyzed the lipophilic precursor to the active dye because the labeling pattern was stable for hours after the loading period and dyes introduced into the cytoplasm during acid loading were retained in the cytoplasm (Fig. 4). Therefore, differences in the subcellular distribution of these dyes after incuba-

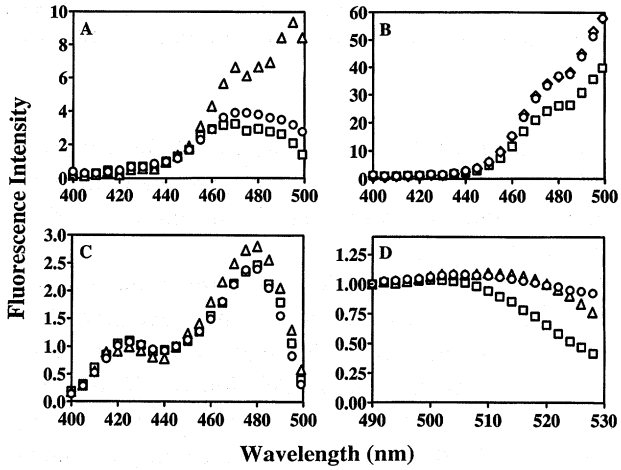

Fig. 5. Comparison of the excitation spectra of fluorescence of roots after incubation with fluorescein based dyes and that of dyes in standard solutions. Roots were loaded with BCECF-AM (**A**), CDCF-DA (**B**, SNARF-1-AM (**C**), and SNAFL-1-DA (**D**) and the excitation spectra of the fluorescence (○) were determined using a PTI FM 2010 microscopy system as described under Material and methods. Excitation spectra of BCECF, SNAFL-1, or SNARF-1 in pH 5 (□) or 7 (△) solutions were also determined using the PTI system. Excitation spectra of CDCF in pH 5 (□) and 6 (△) solutions were also determined. Fluorescence intensities were normalized to 440, 410, 490, and 440 nm for BCECF, CDCF, SNAFL-1, and SNARF-1, respectively

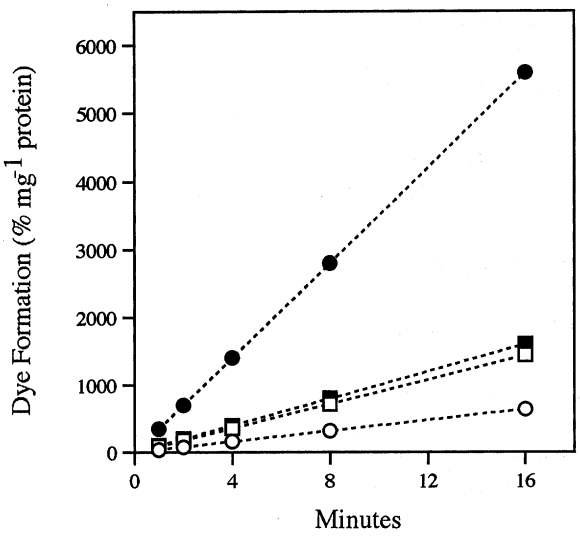

Fig. 6. Time course of SNAFL-1 and BCECF production by crude extracts. Crude extracts were incubated in the presence of 2 μM SNAFL-1-DA (○, □) or BCECF-AM (●, ■) at pH 5.5 (circles) or 7.5 (boxes) and the production of the corresponding dye was followed by changes in fluorescence as described under Material and methods

tion of the tissue with the lipophilic precursors may reflect differences in the subcellular distribution of the esterase activity responsible for the production of active dye molecules. Data to support this hypothesis were pursued by comparing the conversion of BCECF-AM and SNAFL-1-DA to the dyes. These two lipophilic precursors and dyes were chosen because they represented the extreme differences in subcellular distribution. Initially, we tried to produce protoplasts as a source of intact vacuoles to compare the subcellular distribution of esterase activities. Our attempts to use the method of Lin (1980) to produce protoplasts from corn roots were unsuccessful.

Alternatively, the esterase activities in crude extracts at two pH values were compared. The rationale for such an approach was as follows. If a vacuolar esterase was responsible for the conversion of the BCECF-AM to BCECF, then this esterase activity should be more apparent at pH 5.5 than at 7.5. Conversely, if a cytoplasmic esterase was responsible for the conversion of SNAFL-1-DA to SNAFL, then this enzyme activity should be more apparent at pH 7.5 than at 5.5. When crude extracts were incubated with BCECF-AM, more BCECF was produced at pH 5.5 than at 7.5 (Fig. 6). When crude extracts were incubated with SNAFL-1-DA, more SNAFL-1 was produced at pH 7.5 than at 5.5 (Fig. 6).

The substrate dependence of the esterase activities was examined (Fig. 7). Micromolar concentrations of BCECF-AM saturated the enzyme activity that produces BCECF at pH 5.5. Increasing the pH from 5.5 to 7.5 decreased the apparent maximum velocity and increased the apparent Km for BCECF-AM. With SNAFL-1 DA, the production of SNAFL-1 saturated between 3 and 8 μM SNAFL-1-DA at pH 5.5. At pH 7.5, the rates of SNAFL-1 production were consistently greater. However, when the data were transformed and plotted according to a double reciprocal plot, curvilinear functions were obtained. Therefore, a single enzymatic reaction may not be responsible for SNAFL-1-DA conversion to SNAFL-1 at pH 7.5.

In an effort to determine if the same enzyme reactions were responsible for the conversion of BCECF-AM to BCECF as for the degradation of SNAFL-1-DA to SNAFL-1, the rates of esterase activity in the presence of one substrate were compared to that in the presence of both. Because the excitation and emission spectra of these two dyes overlap (Haugland 1992), it was not possible to select conditions to observe the fluorescence of one dye exclusively in the presence of both. However, the fluorometric conditions listed

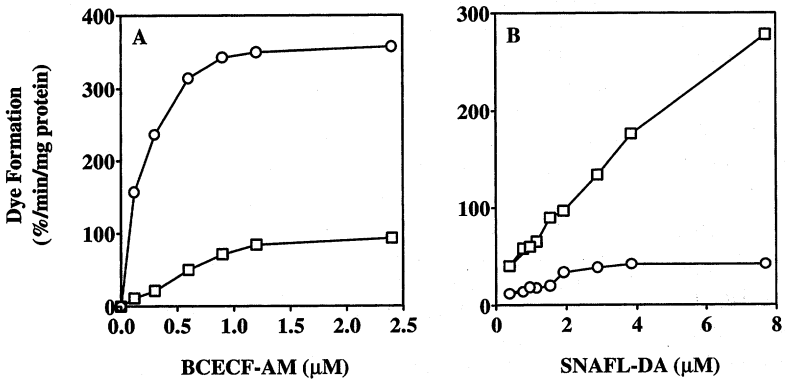

Fig. 7. Substrate dependence for BCECF and SNAFL-1 production. Crude extracts were incubated in the presence of BCECF-AM (**A**) or SNAFL-1-DA (**B**) at pH 5.5 (○) or 7.5 (□) and the production of the respective dye was followed by changes in fluorescence as described under Material and methods

under Material and methods allow one to observe preferentially the production of one dye over the other. Under a variety of conditions (i.e., substrate concentrations and pH), it was observed that the sum of rates of BCECF and SNAFL production in the absence of the other substrate were essentially the same as the rate observed in the presence of both (data not shown). Such results are possible if the two precursors did not mutually compete for the same enzyme. Therefore, two enzymes with differing pH optima were responsible for the removal of blocking groups from BCECF-AM and SNAFL-1-DA.

Discussion

In this report, we have demonstrated that the subcellular distributions of several fluorescein dyes were quite different after root tissues were incubated with their respective lipophilic derivatives (Figs. 2 and 3). These dyes differ significantly in the modification to the fluorescein moiety from which they were derived (Haugland 1992). Both BCECF and CDCF, which were localized predominantly in the vacuoles, contain an additional ring structure adjacent to the fluorescein moiety (Haugland 1992). The influence of this additional conjugated carbon ring to the subcellular localization of the dye merits further investigations. Because the labeling patterns of SNARF-1-AM and BCECF-AM, and SNAFL-1-DA and CDCF-DA were different, molecular structures other than the blocking groups of the carboxylic acid contributed to the metabolism of these different molecules in root epidermal cells.

When the dyes were introduced into the cytoplasm by acid loading, the dyes were retained in this compartment hours after the loading process (Fig. 4). These results indicate the dyes were not readily redistributed from the cytoplasm to the vacuole. In addition, epidermal cells did not become fluorescent when roots were incubated in the presence of free dyes at neutral external pH (data not shown). Therefore, there is no evidence in this report to support Oparka's (1991) hypotheses to account for vacuolar accumulation of hydrophilic dyes by fluid-phase endocytosis or carrier mediated transport across on the tonoplast membrane.

The comparison of the esterase activities responsible for the conversion of BCECF-AM to BCECF and SNAFL-1-DA to SNAFL-1 indicated that different enzymatic activities were responsible for these conversions. The characteristics of these esterase activities were consistent with the subcellular distribution of the dyes in the tissue (Figs. 6 and 7). However, further experimentation is necessary to fully understand how these esterase activities may influence the intracellular compartmentation of lipophilic dye precursors.

Acknowledgement

Mentioning of a brand name does not constitute an endorsement by USDA over other products.

References

Bensadoun A, Weinstein D (1976) Assay of proteins in the presence of interfering materials. Anal Biochem 70: 241–250

Boller T, Kende H (1979) Hydrolytic enzymes in the central vacuole of plant cells. Plant Physiol 63: 1123–1132

Brauer D, Ott J, Tu S-I (1995) Selective accumulation of BCECF in vacuoles of maize root tip cells. J Plant Physiol 145: 57–61

Bush DS, Jones RL (1990) Measuring intracellular Ca^{2+} levels using fluorescent probes, indo-1 and fura-2. Plant Physiol 93: 841–845

Cork RJ (1986) Problems with application of Quin-2-AM to measuring cytoplasmic free calcium in plant cells. Plant Cell Environ 9: 157–161

Dixon GK, Braunte C, Mernett, NJ (1989) Measurement of internal pH in coccolithoph. *Emiliana huxlexi* using 2′,7′-bis-(2-carboxyethyl)-5-(and-6)carboxyfluorescein acetoxymethyl ester and digital imaging microscopy. Planta 178: 443–449

Haugland RP (1992) Handbook of fluorescent probes and research chemicals. Molecular Probes Inc., Eugene, OR

Kurkdjain A, Guern J (1981) Vacuolar pH measurement in higher plant cells. I. Evaluation of the methylamine method. Plant Physiol 67: 953–957

– – (1989) Intracellular pH: measurement and importance in cell activity. Annu Rev Plant Physiol 40: 271–303

– Quiquampox H, Barbier-Brygoo H, Pean M, Manigault P, Guern J (1985) Critical examination of methods for estimating the vacuolar pH of plants cells. In: Marin BP (ed) Biochemistry and function of vacuolar ATPase in fungi and plant cells. Springer, Berlin Heidelberg New York Tokyo, pp 98–113

Lawrence ME, Possingham JV (1986) Direct measurement of femtogram amounts of DNA in cells and chloroplasts by quantitative microspectrofluorometry. J Histochem Cytochem 34: 761–767

Lin W (1980) Corn root protoplasts, isolation and general characterization of ion transport. Plant Physiol 66: 550–554

Nagahashi G, Baker AF (1984) B-glucosidase activity in corn root homogenates: problems in subcellular fractionation. Plant Physiol 72: 837–846

Nelson N, Taiz L (1989) The evolution of H^+-ATPases. Trends Biochem Sci 14: 114–116

Oparka KJ (1991) Uptake and compartmentation of fluorescent probes in plant cells. J Exp Bot 238: 565–579

Pfeffer PE, Tu S-I, Gerasimowicz WC, Boswell TR (1987) Effects of aluminum on the release and/or immobilization of soluble phosphate in corn root tissue: a ^{31}P nuclear magnetic resonance study. Planta 172: 200–208

Raven JA, Smith FA (1979) Intracellular pH and its regulation. Annu Rev Plant Physiol 30: 289–311

Roberts JKM, Ray PM, Wade-Jardetzky N, Jardetzky O (1981)

Effect of Nikkomycin Z, a chitin-synthase inhibitor, on hyphal growth and cell wall structure of two arbuscular-mycorrhizal fungi

B. Bago[1,*], **H. Chamberland**[2], **A. Goulet**[2], **H. Vierheilig**[1], **J.-G. Lafontaine**[2], and **Y. Piché**[1]

[1] Centre de Recherche en Biologie Forestière, Faculté de Foresterie et de Géomatique, and [2] Département de Biologie, Faculté des Sciences et de Génie, Université Laval, Sainte-Foy, Québec

Received August 22, 1995
Accepted January 30, 1996

Summary. Different concentrations of Nikkomycin Z, a competitive inhibitor of chitin-synthase, were applied to the arbuscular-mycorrhizal fungi (AMF) *Gigaspora margarita* and *Glomus intraradices* under in vitro conditions. These two fungi are known to differ in the structure and composition of their cell wall. The two AMF were able to grow in the presence of a higher concentration of this antibiotic than so far reported for other fungi. Fluorescence, electron microscopic and cytochemical studies showed that the blocking of the fungal chitin-synthase activity induces alterations in hyphal morphology, a reduction in fungal wall thickness, and several other changes in the hyphal wall structure and organization. The possible role of chitin-synthase in the hyphal growth and morphogenesis of these symbiotic fungi and its putative regulation by the host plant during the symbiosis are discussed.

Keywords: Arbuscular-mycorrhizal fungi; Chitin; Chitin-synthase; Fungal cell wall; Fungal morphogenesis; Nikkomycin Z.

Abbreviations: AM arbuscular mycorrhiza; AMF arbuscular-mycorrhizal fungus; DAPI 4′-6-diamidino-2-phenylindole; MIC minimal inhibitory concentration; NAG N-acetylglucosamine; TEM transmission electron microscopy; T50, T5, T0.5 treatments with different Nikkomycin Z concentrations (50 µg/ml, 5 µg/ml, 0.5 µg/ml); UDP-NAG uridine-diphosphate-N-acetylglucosamine; WGA wheat germ agglutinin.

Introduction

Numerous studies have focused on the fungal cell wall in recent years. This structure constitutes a physical and chemical barrier which isolates the fungal cytoplasm from its environment and permits these organisms to resist adverse external conditions. Different aspects concerning fungal cell walls have been investigated, i.e., their morphology and composition as taxonomic parameters (Bartnicki-Garcia 1987), their antigenic properties (Cassone 1986), their role in fungal morphogenesis and apical growth (Reinhardt 1892, Wessels 1994) as well as their behaviour during the process of protoplast formation and regeneration (Peberdy 1979, Elorza et al. 1987). The role of the fungal cell wall in the regulatory mechanisms of plant-fungal interactions has also been the subject of many studies (Hadwiger et al. 1986, Bonfante-Fasolo 1987, Ebel and Cosio 1994).

Arbuscular-mycorrhizal fungi (AMF) are microorganisms which establish a mutualistic symbiosis with the roots of about 90% of all land plants (Harley and Smith 1983). They are considered to be Zygomycetes, although their taxonomic position is still a matter of discussion (Simon et al. 1993, Franke and Morton 1994, Gianinazzi-Pearson et al. 1994). Similar to other fungi in the Zygomycotina group (Lewis 1991), AMF possess chitin as one of their principal cell wall components (Bonfante-Fasolo and Grippiolo 1984, Grandmaison et al. 1988, Bonfante et al. 1990, Gianinazzi-Pearson et al. 1994). However, their hyphal wall structure and composition does not show a uniform pattern, as they differ between genera (Gianinazzi-Pearson et al. 1994, Giovannetti and Gianinazzi-Pearson 1994) as well as between the different developmental stages of the fungus (Bonfante-Fasolo and Grippiolo 1982, Grandmaison et al. 1988, Bonfante-Fasolo et al. 1990). In fact, the AMF cell wall exhib-

* Correspondence and reprints: Centre de Recherche en Biologie Forestière, Faculté de Foresterie et de Géomatique, Pavillon C.E. Marchand, Université Laval, Sainte-Foy, Que. G1K 7P4, Canada.

Extent of intracellular pH changes during H^+ extrusion by maize root-tip cells. Planta 152: 74–78

– – – – (1980) Estimation of cytoplasmic and vacuolar pH in higher plant cells by ^{31}P NMR. Nature 283: 870–872

Rost FWD, Shepherd VA, Ashford AE (1995) Estimation of vacuolar pH in actively growing hyphae of the fungus *Pisolithus tinctorius*. Mycol Res 99: 549–553

Sakano K, Yazaki Y, Mimura T (1992) Cytoplasmic acidification induced by inorganic phosphate uptake in suspension cultured *Catharanthus roseus* cells. Measurement with fluorescent pH indicator and ^{31}P-nuclear magnetic resonance. Plant Physiol 99: 672–680

Slayman CL, Moussatos VV, Webb WW (1994) Endosomal accumulation of pH indicator dyes delivered as acetoxymethyl esters. J Exp Biol 196: 419–438

Sze H (1985) H^+-translocating ATPases: advances using isolated vesicles. Annu Rev Plant Physiol 36: 175–208

Tu S-I, Loper M, Brauer D, Hsu A (1992) The nature of proton translocating ATPases in maize roots. J Plant Nutr 15: 929–944

Yin Z-H, Heher U, Raghavendra AS (1993) Light-induced changes in leaves of C4 plants. Comparison of cytosolic alkalination and vacuolar acidification with that of C3 plants. Planta 189: 267–277